AN INVESTIGATION OF A HOVERING ROTOR IN GROUND EFFECT

A. Graber, A. Rosen, and A. Seginer
Faculty of Aerospace Engineering
Technion - Israel Institute of Technology
Haifa 32000, Israel.

Abstract

A new free-wake aerodynamic model of a rotor hovering in ground effect is briefly presented. Then the model is validated by comparing the numerical results with existing experimental data. Very good agreement of the thrust coefficient is obtained, whereas discrepancies in the torque coefficients are discussed. After validation, the numerical characteristics of the model are investigated. The convergence between consecutive iterations and convergence with respect to different parameters that define the model, are presented and discussed. At the end of the paper the capabilities of the model are shown by considering various aspects of the ground effect.

List of Symbols

- c - blade chord (constant in all the examples)
- C_Q - torque coefficient ($Q/\rho\pi R^5\Omega^2$)
- C_T - thrust coefficient ($T/\rho\pi R^4\Omega^2$)
- F.M - the rotor Figure of Merit
- h - height above the ground
- L' - blade lift per unit length
- l - blade-section loading ($L'/\rho R^3\Omega^2$)
- N_r - number of columns of cells along the blade
- N_R - number of vortex rings that form the far wake
- N_b - number of blades
- Q - rotor torque
- R - rotor radius
- T - rotor thrust
- r - radial coordinate
- r_{co} - radial coordinate of the blade root
- v_T - tip speed
- z - axial coordinate (measured downward from the plane of rotation)
- α - angle of attack
- θ - sectional pitch = $\theta_o - \theta_{TW}(r/R)$
- ρ - air mass density
- ϕ_{NW} - azimuthal length of the near wake
- ψ - azimuth angle behind the trailing edge
- Ω - rotor rotational speed
- $(\,)_\infty$ - a variable out of ground effect

Introduction

The ground effect is a well-known and widely used phenomenon in the daily operations of helicopters. The ground effect decreases rapidly as the height above the ground is increased. In a forward flight at a constant altitude the ground effect decreases rapidly as the airspeed is increased.

Ground effect has been investigated quite extensively during the years because of its importance. The research included both theoretical and experimental investigations. Most of the research of this phenomenon concentrated on the hovering case because of the intensity and importance of the ground effect in hover. The interested reader may find a more detailed literature survey of the ground effect in (Ref. 1).

It is well-known that in order to calculate accurately the aerodynamic behavior of a hovering rotor it is necessary to know the geometry of the rotor wake. This geometry can be assumed, based on physical reasoning or empirical data. It is, however, preferable to obtain this geometry as part of the solution procedure. The geometry is determined by the vorticity conservation laws that require that the vortex elements that form the wake be force free. This analysis which is therefore referred to as a "free wake analysis" poses a complicated nonlinear problem because of the highly nonlinear mutual interdependence of the wake geometry and the aerodynamic loads over the blades.

An accurate treatment of the entire wake of the rotor requires computing resources that are so large that they render it impractical. An approximation must therefore be used to save computing resources. The influence of the wake on the rotor loads decreases rapidly as its distance from the rotor increases. It is, therefore, customary to divide the wake into near and far regions in which different levels of numerical accuracy are employed. An example of such a model is presented in (Refs. 2,3). The near wake which strongly influences the wake is modeled accurately, but the

modeling of the far wake includes several simplifications that result in significant reductions in the required computing resources. When a rotor hovers out of the ground effect (OGE) it is customary to assume that the helical vortex filaments that form the far wake, have a constant radius and pitch. A further simplification of this structure is its replacement by a uniform distribution of identical vortex rings, or by a semi-infinite vortex cylinder. It is obvious that these simplifications of the far wake do not apply to the wake of a rotor in ground effect (IGE), where the radius of the helical vortex filaments continues to increase while their downward axial velocity decreases.

Thus a free wake analysis of an IGE hovering rotor is consequently much more complicated than a rotor hovering OGE. This probably explains why free-wake models of rotors hovering IGE are not available, whereas good free-wake models of rotors hovering OGE were presented in the past. Reference 1 gives a detailed description of numerical models of rotors IGE. A representative example of a relatively recent research is the model of Saberi (Ref. 4) which is based on a non-linear vortex description that was previously suggested by DuWaldt (Ref. 5). The wake of Saberi's model includes only two vortex filaments: one is the tip vortex and the other starts at an inner section of the blade. The circulation around the vortex line that represents the blade is determined, based on experimental results, and is kept constant throughout the entire calculation procedure that centers on the wake geometry generated by a given load distribution. The complete problem of determining the aerodynamic loads over the blades and the corresponding wake geometry of a given rotor hovering IGE, was not addressed. Somewhat later, Saberi (Ref. 6) raised the idea of using a super computer for the solution of even this simplified model because of the extremely large computer resources that it required.

A free-wake model, capable of dealing with the complete problem of a rotor hovering IGE, was developed recently (Ref.7). This model considerably reduced the required computer resources, while the accuracy did not deteriorate. This model is described in detail in Ref. 1. Therefore, only details that are necessary for the completeness of this paper will be presented. The assumptions and simplifications of this model must be validated. Validation of the model in Ref. 1 was limited. It is therefore validated further here by a comparison of numerical and experimental results. A subsequent study of the numerical properties of the model concentrates on the convergence properties of the model and on their dependence on several model parameters. Finally the capability of the model is demonstrated by a study of various aspects of the ground effect.

The Mathematical Model - A Brief Description

The new model uses a nonlinear vortex-lattice method (VLM). It is described in detail in Ref. 1. Following is a brief description that is necessary for the completeness of this paper.

The problem at hand is axisymmetric and quasi-steady. All the blades experience identical conditions that are steady in the frame of reference of the blade. The examination of a single representative blade is therefore sufficient. Each blade is divided into cells for the discretization of the vorticity distribution. (N_r+1) cross sections along the span of the blade, with the first section at the blade root and the last at the blade tip, define N_r columns of cells. Each column is further divided along its chord into more cells. A control point inside each cell is defined at the usual three-quarters point of the middle chord of the cell. The flow tangency condition is satisfied at all the control points.

The vorticity that is distributed over each cell is represented by a "bound vortex", which is a vortex filament along the quarter chord of the cell. In accordance with the circulation conservation laws, two bound trailing vortex filaments run along the two sides of each cell's column, from the bound-vortex filament to the trailing edge, and continue from there into the wake as free trailing vortices.

The wake is divided into two regions: the near wake and the far wake.

The near wake begins at the trailing edge of the blade and terminates at an azimuthal distance ϕ_{NW} from the trailing edge. ϕ_{NW} is an input to the model. There are (N_r+1) vortex filaments trailing behind each blade. In the near wake these vortex filaments are modeled as chains of straight segments of vortex elements. The basic geometry of the filaments is that of a concentric helix, but it is deformed by the mutually- and self-induced velocities, because the vortex filaments must be force free and follow streaklines.

Experiments as well as calculations (see for

example Refs. 2,3), show that the near wake tends to roll-up and form two concentrated vortices: a root vortex and a tip vortex. The model simulates the wake roll-up by gathering the vortex filaments at the end of the near wake into two groups that form the tip and root vortices. These two vortices constitute the far wake.

Most of the deformation of the wake of a rotor hovering OGE occurs in the near-wake region, so that the far-wake geometry can be prescribed after the near-wake geometry is known. This is not the case when the rotor is hovering IGE, where the wake continues to deform as it approaches the ground. A simulation of a continuously deforming wake would be unacceptable as far as the required computer resources are concerned. Further simplifications are therefore needed in addition to the reduction of the wake to root and tip vortices only.

The basic geometry of the tip vortex in the far wake is a variable helix with an increasing radius and a decreasing pitch, as it approaches the ground. In the present model this helix is replaced by a system of vortex rings. Each filament revolution is replaced by N_b vortex rings where N_b is the number of blades. The spacings between the rings and their radii are determined during the solution procedure after applying the condition that the far wake is force free (a free far wake). The root vortices in the far wake also are approximated by a series of vortex rings, but their influence on the loads on the blades is usually quite small.

The ground is represented by imaging of the whole vortex system including the bound vortices, the near wake vortex filaments and the far wake rings of all the blades. The imaging satisfies automatically the tangency condition on the ground but also doubles the magnitude of the problem at the same time.

The accuracy of the description of the vortex filaments is improved by a vortex-core model applied to the near and far wakes. This model also prevents the singularities in the computation of the self-induced velocities.

The model described above is highly nonlinear and contains a relatively high number of different parameters. A converged solution has therefore to be reached by an iterative procedure. The convergence applies to both the circulation around the vortex filaments and the entire wake geometry. Once the solution is converged the aerodynamic loads on the blades are obtained from the Kutta-Jukowski equation plus the influence of the profile drag.

Results and Discussion

Table 1 presents the details of four rotors. These rotors were chosen because the available experimental data on their behavior IGE can be used to validate the present numerical model. Rotor No. 1 will be referred to here only very briefly. Rotors nos. 2 and 3, tested by Koo and Oka (Ref. 8), are identical except for different pitch settings, θ_0, at the root of the blades. This rotor has three blades with a linear pretwist of -8.3°. Rotor no. 4, tested by Knight and Hefner (Ref. 9), has two flat blades (zero pretwist). All the rotors have similar rotational speeds with tip velocities that do not exceed 100 m/sec. Compressibility effects can, therefore, be neglected.

The results presented here were obtained with a cell distribution over the blades that has just one cell in the chordwise direction. Studies (Refs. 2,3) have shown that a chordwise division into cells does not influence the wake geometry or the distribution of aerodynamic loads over the blades, and is needed only when a refined prediction of the chordwise load distribution is required. Also, the cell distribution can be refined in the chordwise direction after the calculations with one chordwise cell converge. This technique significantly reduces the CPU time. Most of the results presented here were obtained (unless otherwise stated, see Table 2) with eight cells in the spanwise direction along the blade. The nondimensional radial coordinates of the cross sections that define the cells (specified by their dimensional radii divided by the rotor radius) are: $\tilde{r}_{co}$, 0.4, 0.6, 0.75, 0.85, 0.8, 0.95, 0.975, 1. A more refined distribution of cells is used in the tip region where the aerodynamic loads vary rapidly in the spanwise direction.

A length of 450° was chosen for the near wake of the two-bladed rotors and of 300° for the three-bladed rotors, to allow the passage of two consequent blades over the near wake. The far wake is represented in most of the cases by 15 vortex rings. Each vortex ring represents $(1/N_b)$ revolutions of the far wake. The length of the far wake is, therefore, 2100° for rotors 2 and 3, and 3150° for rotors 1 and 4. Several cases were calculated with 25 vortex rings in the far wake (Table 2) that represent lengths of 4950° and 3300°, for the two and three-bladed rotors, respectively.

Table 1 - The properties of the rotors

Rotor No.	Source	R [m]	c [m]	r_{co} [m]	V_T [m/sec]	Ω [rad/sec]	Θ_{TW} [°/m]	θ_o [°]	N_b [-]
1	Sharpe (1986) Ref. 8	0.962	0.0864	0.0951	100.7	104.7	0	10	2
2	Koo & Oka (1971) Ref. 9	0.550	0.033	0.0825	59.3	107.9	-8.3	11.25	3
3	Koo & Oka (1971) Ref. 9	0.550	0.033	0.0825	59.3	107.9	-8.3	16.25	3
4	Knight & Hefner (1941), Ref. 10	0.762	0.0508	0.1270	71.8	94.3	0	10	2

Table 2 - The numerical results

Case No.	h/R	C_T	C_Q	F.M.	N_R	MTPI [min]*
1	0.396	0.00680	0.000380	0.757	25	5.67
1a	∞	0.00557	0.000370	0.764	25	3.15
2	1	0.00257	0.000129	0.565	15	2.15
2a	∞	0.00247	0.000129	0.567	15	1.52
2b	∞	0.00241	0.000129	0.568	25	4.56
2c	2	0.00249	0.000129	0.566	15	3.42
2d	2	0.00243	0.000129	0.567	25	9.17
2e	0.5	0.00291	0.000127	0.554	15	1.72
2f	0.2	0.00351	0.000122	0.502	15	3.02
3	1	0.00596	0.000379	0.777	15	1.54
3a#	1	0.00596	0.000378	0.779	15	2.52
3b	1	0.00595	0.000379	0.778	25	3.15
3c	∞	0.00574	0.000375	0.779	15	2.44
3d	∞	0.00575	0.000375	0.780	25	4.56
3e	0.5	0.00641	0.000376	0.761	15	1.81
3f	1.5	0.00581	0.000374	0.775	15	2.39
4	1	0.00482	0.000281	0.745	15	1.76
4a	∞	0.00451	0.000285	0.758	15	1.72
4b	∞	0.00451	0.000285	0.758	25	3.16
4c	2	0.00452	0.000285	0.759	15	1.19
4d	0.5	0.00538	0.000273	0.705	15	2.60

*Mean time per iteration on an IBM 3081D
#Fifteen cells along each blade

The results of the calculations are presented in Table 2. Each rotor was represented by several cases. Each case is designated by a Latin letter that is added to the rotor number. Usually these cases represent different heights above the ground, but in certain cases they represent variations in the number of vortex rings that form the far wake or the number of cells over the blade. Table 2 presents for each case the final (at the end of the 20th iteration) thrust coefficient-C_T, the torque coefficient-C_Q, the Figure of Merit-(F.M.) and the mean CPU time per iteration-MTPI. As convergence is approached, the required CPU time per iteration decreases. Usually the actual CPU time of each of the last iterations is reduced, in comparison to the first iterations, by a factor of two or even three.

Validation of the model

The main influence of the ground is the overall reduction of the induced axial velocities in the frame of reference of the rotating blades. Good agreement between the calculated and measured induced velocities, OGE and IGE, was obtained for rotor no. 1 and was presented in Ref. 1. The reduction in the induced axial velocities causes a reduction in the sectional inflow angles, which are the angles between the sectional resultant velocity and the plane of rotation. With a constant pitch angle of the blade, the sectional effective angle of attack increases as the ground is approached. The spanwise distributions of the sectional angle of attack for rotor no. 3, OGE and at a height of half a radius, are presented in Fig. 1. It is shown that the angle of attack is considerably increased by the ground effect, except for a small region near the tip.

The larger the angle of attack over most of the cross sections results also in a larger thrust. The ratio between the thrust coefficients in and out of ground effect, is presented in Figs. 2a-c, as a function of the height of the rotor above the ground. The agreement between the experimental and the calculated results is very good, except for rotor no. 3 at heights less than three quarters of a radius. Rotor no. 3 has larger attack angles than rotor no. 2. These are increased even more by the ground effect at small heights (Fig. 1) resulting in large parts of the blade being stalled, and in the reduction of the actual thrust which the inviscid aerodynamics cannot predict. Indeed Koo and Oka (Ref. 8) detected, by flow visualization, flow separation over the inner parts of the blade, that started at a height of 0.7 radius above the ground and grew rapidly as the height decreased.

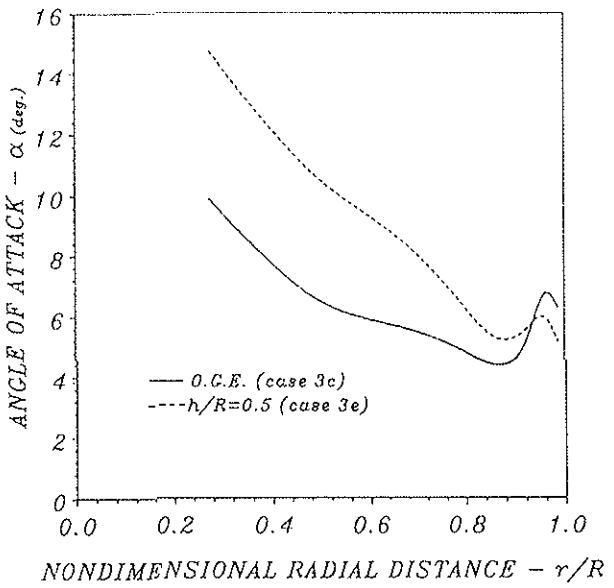

Fig. 1 - Spanwise distribution of the sectional angle of attack, IGE and OGE, for rotor no. 3.

It is interesting to note that the thrust ratio at a height of half a radius, calculated by the present model, agrees well with the predictions of Ref. 8 which were based on trends of experimental data that were not affected by stall. If necessary, stall corrections can be incorporated into the present inviscid model.

The influence of the ground effect on the torque of the rotor is more complicated because it includes two contradicting effects. On the one hand, the sectional lift is larger because of the increased angles of attack, thus increasing the sectional induced drag and consequently also the rotor torque coefficient. On the other hand, the reduced cross sectional inflow angle reduces the induced drag and with it also the rotor torque coefficient. The two contradicting effects are of the same order of magnitude. Therefore, the influence of the ground on the torque coefficient which is the sum of the two, is less pronounced than on the thrust coefficient. Moreover, the ground effect may even act in opposing directions at different heights as a result of different relative intensities of the two contradicting effects. The ratio between the torque coefficients in and out of ground effect, of rotors nos. 2-4, is presented in Figs. 3a-c, respectively, as functions of the height above the ground. In general, as expected, the influence of the ground on the torque is much smaller than its influence on the thrust. Furthermore, the nature of the ground effect on different rotors is not identical and may even change on a certain rotor as the

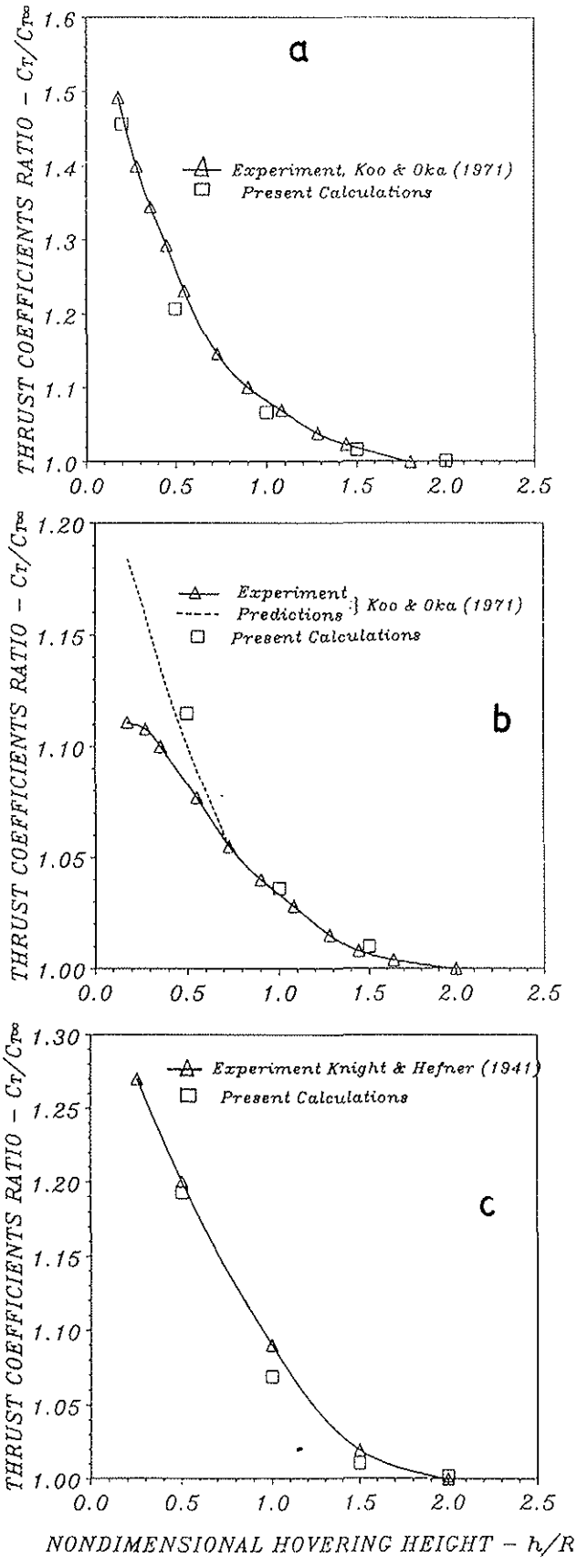

Fig. 2 - The influence of the ground on the rotor thrust as a function of the rotor height above the ground. (a) Rotor no. 2, (b) Rotor no. 3, (c) Rotor no. 4.

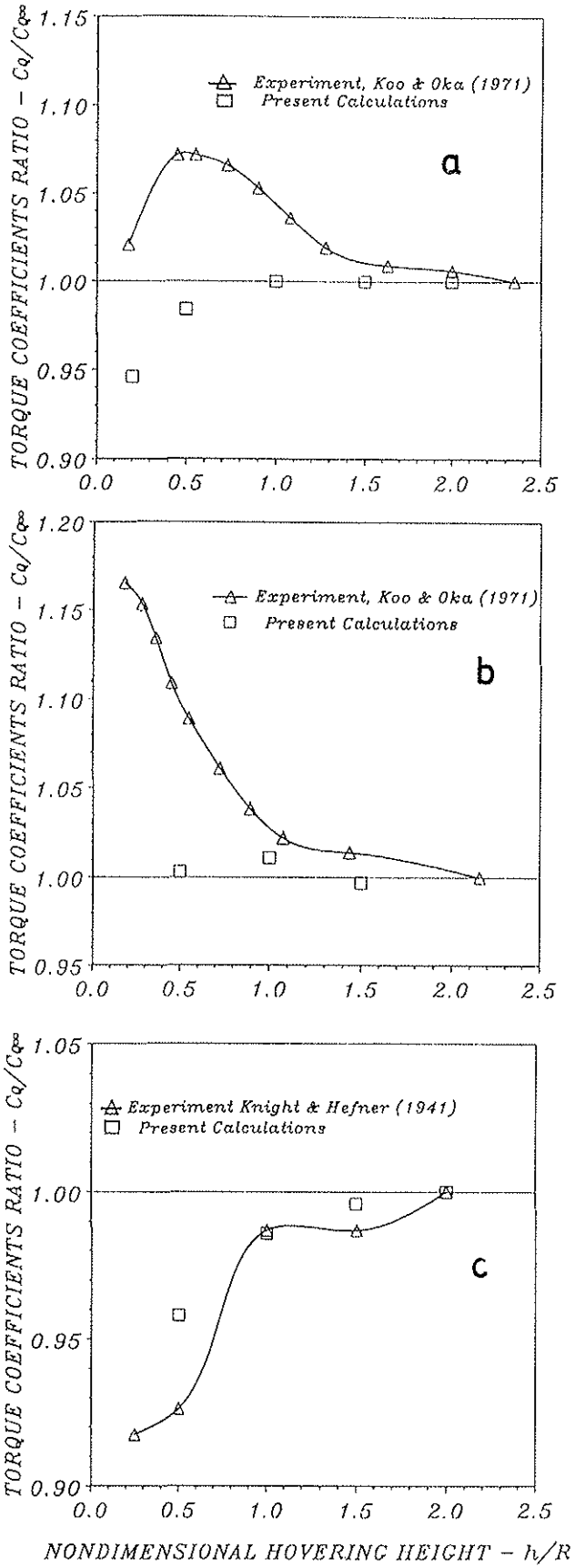

Fig. 3 - The influence of the ground on the required torque. (a) Rotor no. 2, (b) Rotor no. 3, (c) Rotor no. 4.

ground is approached. The present model predicts for rotor no. 2 a negligible ground effect at heights above half a radius (Fig. 3a). At smaller heights the torque decreases rapidly. This decrease in the torque below h/R=0.5 was also observed experimentally. However, the experiments also show an increase of more than seven percent in the required torque between heights of two radii and one half radius, not predicted by the numerical model. On rotor no. 3 (Fig. 3b) relatively large increases in the torque are measured at heights lower than one radius, that also are not predicted numerically. The increased torque can be attributed, at least partially, to stall effects which (as indicated above) become important at such heights. The experimental behavior of the required torque of rotor no. 4 differs completely from that of the other two rotors (Fig. 3c). A considerable reduction is presented in the required torque of rotor no. 4 as the height is decreased, without any previous increases. This behavior is also predicted numerically fairly well. Zbrozek (Ref. 11) also was aware of the contradicting results presented by different researchers, concerning the influence of the ground proximity on the required torque at fixed pitch. It seems that thirty years later further investigation is still required to clarify this problem.

The Convergence of the Numerical Model

The convergence problem has two aspects. One is the convergence of consequent iterations. The other is the effect of the various parameters that define the numerical model on the converged solution.

The convergence of the thrust coefficient-C_T, torque coefficient-C_Q, and the figure of merit-F.M., as functions of the iteration number, is presented in Figs. 4-6, respectively. These figures refer to case 3b where rotor no. 3 hovers at a height of one radius. Good convergence is shown, with the thrust coefficient being the slowest to converge. As indicated above, and as also obtained in other cases, the 20th iteration represents a converged solution. The variables that are shown in Figs. 4-6 are the results of an integration over the entire rotor. Local rotor variables, such as the sectional angle of attack or the sectional loading, also show good convergence characteristics. Another very useful measure of the convergence is the wake geometry and it too converges well in all the cases.

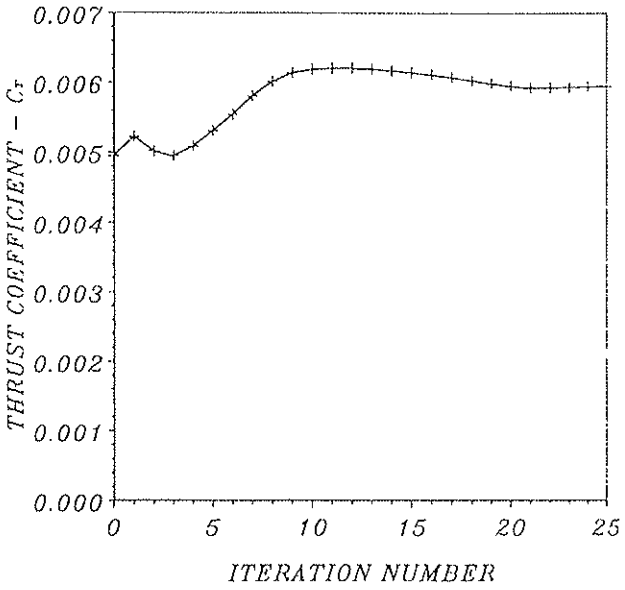

Fig. 4 - The iterative convergence of the thrust coefficient - case 3b, h/R=1.

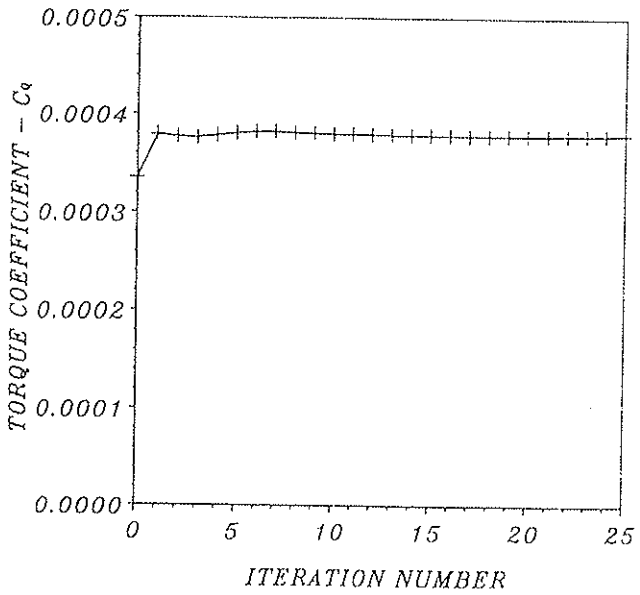

Fig. 5 - The iterative convergence of the torque coefficient - case 3b, h/R=1.

As mentioned above, in addition to the iterative convergence there is also the question of the effect of the parameters that define the numerical model on the converged solution. Such a parameter, for example, is the number of cells over the blade. As previously explained, most of the cases here have eight cells along each blade. In order to investigate the effect of this parameter on the converged solution a few cases with 15 cells also were calculated. As indicated in Table 2, cases 3 and 3a deal with rotor no. 3 at a height of one

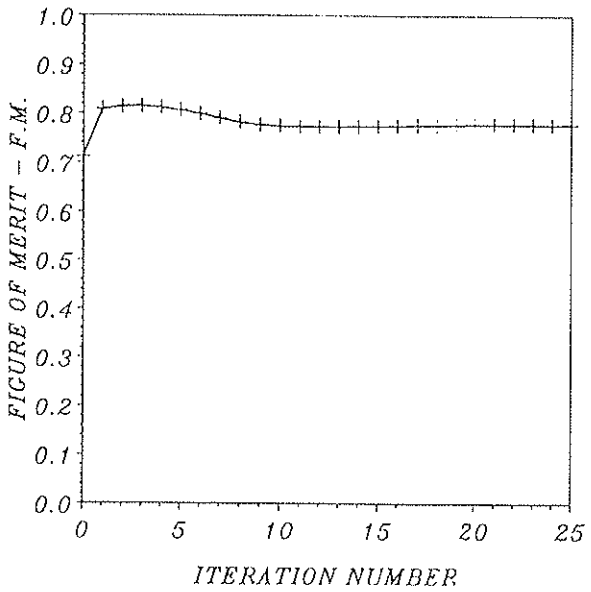

Fig. 6 - The iterative convergence of the Figure of Merit - case 3b, h/R=1.

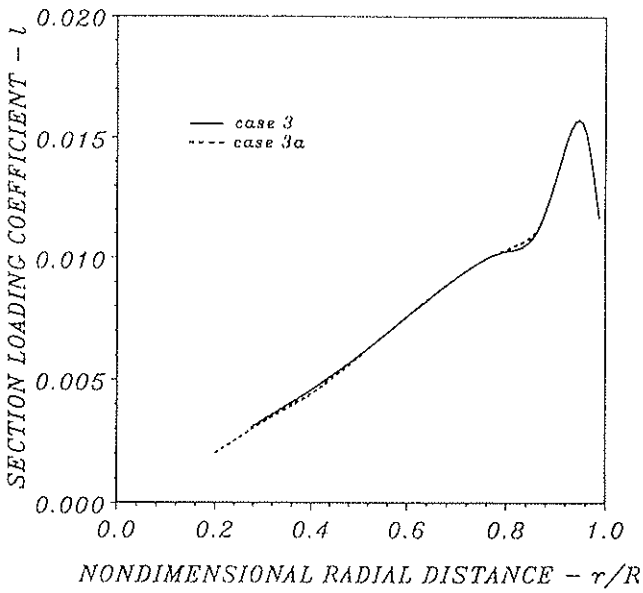

Fig. 7 - The influence of the number of cells on the converged solution - case 3 with 8 cells and case 3a with 15 cells.

radius above the ground, with the far wake represented by 15 vortex rings. The only difference between the two cases is the number of cells along the blade which is 8 and 15, respectively. The nondimensional radial position of the cross sections that define the fifteen cells in case 3a are: $\tilde{r}_{co}$, 0.25, 0.35, 0.45, 0.5, 0.55, 0.6, 0.65, 0.7, 0.75, 0.8, 0.85, 0.9, 0.95, 0.975, 1.

A comparison of the spanwise distributions of the loading coefficient, as obtained in cases 3 and 3a, is presented in Fig. 7. Almost doubling the number of cells along the blade results in only negligible differences. On the other hand, as can be seen in Table 2, the required CPU time was considerably increased.

Another parameter which may have an important effect on the convergence is the number of vortex rings that form the far wake. 15 rings were used in most of the cases presented here. However, results of computations with 25 vortex rings (cases 2b, 2d, 3b, 3d, 4b) were compared with their counterparts with 15 rings (2a, 2c, 3, 3c, 4a, respectively), in order to evaluate their effect. Table 2 indicates that in most of the cases the addition of vortex rings only results in a large increase in the CPU time without any practical change in the results. Only in the case of rotor no. 2 out of ground effect (at a height of two radii the influence of the ground effect is negligible), was some influence of the larger number of rings found (Fig. 8a). At lower heights this influence disappeared. The reason for the influence of the number of rings on the wake geometry of rotor no. 2, as compared with the other rotors, is that this rotor operates at much lower thrust coefficients than the other rotors (see Table 2). Therefore, the induced velocities in this case are smaller and the wake stays closer to this rotor. This effect is shown very clearly in Figs. 8a,b. Cross sections of the wake are presented in these figures. Significant differences between the wake geometries of cases 2a and 2b (Fig. 8a) develop within a distance of less than one radius from the plane of rotation. In cases 3c and 3d (Fig. 8b) the differences between the wake geometries are smaller and occur at larger distances from the rotor. As the height of the rotor above the ground decreases the wake widens rapidly and the influence of the far vortex rings vanishes, even in the case of rotor no. 2.

Further Results

The most significant ground effect is on the wake geometry. The geometry of the tip vortex, which is the most important component of the wake, is shown in Figs. 9a-c. Figure 9a shows that the wake immediately beneath the plane of rotation, contracts as do the wakes OGE. This contraction is the reason for the sharp increase in the section loading near the tip (Fig. 7). After the initial contraction the wake begins to expand because of the ground effect (Fig. 9a). First the expansion is slow, but after two revolutions of the wake, as it approaches the ground, it widens rapidly. The accompanying axial position of the tip-vortex elements is shown in Fig. 9b. After two wake

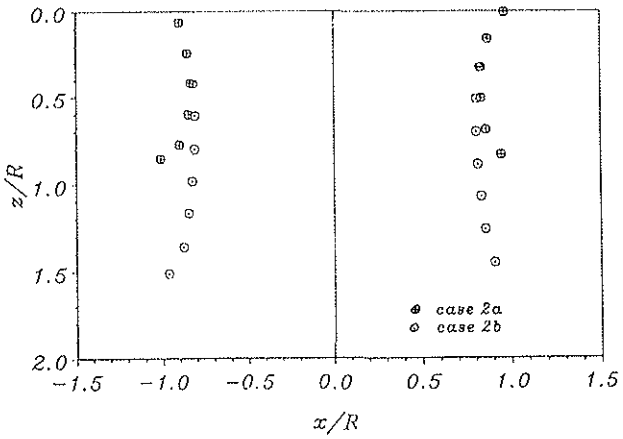

a

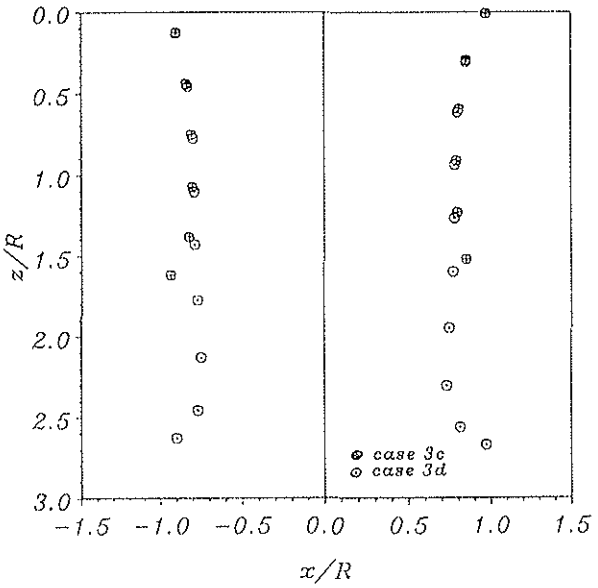

b

Fig. 8 - The effect on the wake geometry of a rotor OGE, of 15 and 25 vortex rings in the far wake. (a) Rotor no. 2, (b) Rotor no. 3.

revolutions, as the tip vortex approaches the ground to a distance of 20% of a radius, its axial velocity decreases rapidly as the wake expands rapidly. Another way of presenting the tip vortex geometry by using a vertical cross section of the wake is shown in Fig. 9c. It too shows first its contraction and then its rapid expansion close to the ground.

An interesting problem is the influence of the blade twist on the ground effect. This problem was discussed previously (Ref. 12) based on empirical data that showed a significant influence. Previous theoretical models were not capable of addressing this problem. In order to show the capability of the present model, rotor no. 2 (which has a twist

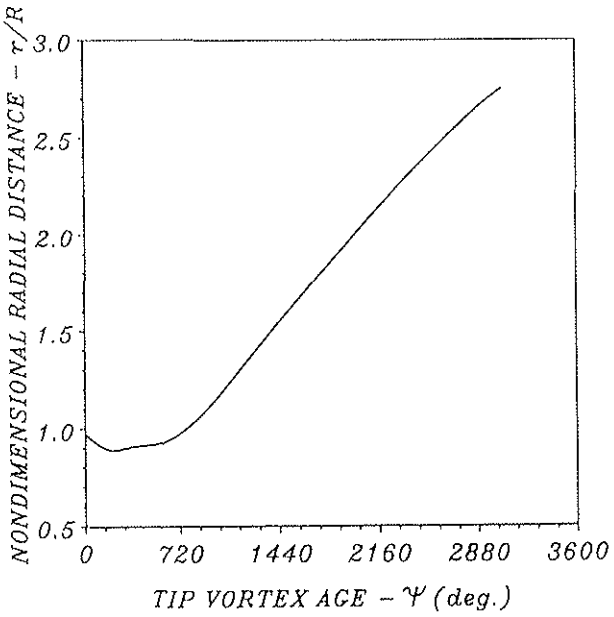

a

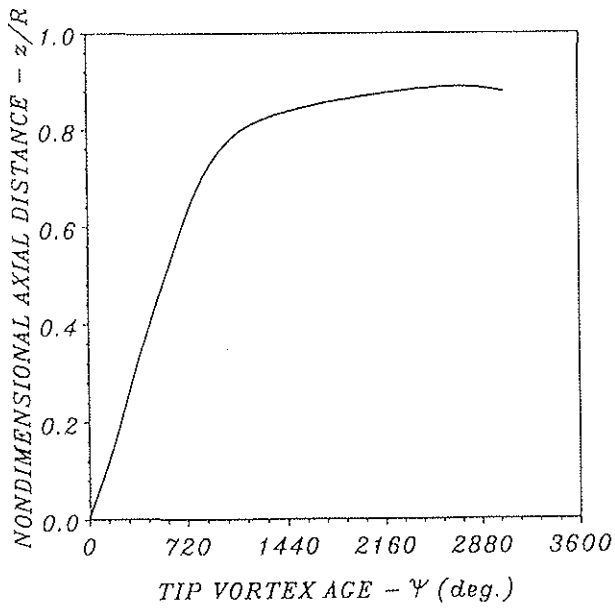

b

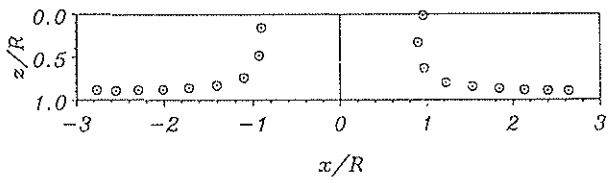

c

Fig. 9 - The geometry of the tip vortex - case 3b, h/R=1. (a) The radial position. (b) The axial position. (c) A vertical cross section of the wake.

of -8.3°) is compared with a rotor that is idential except for zero twist (flat blades). The pitch angle of that rotor was chosen so that OGE it has the same thrust as rotor no. 2. As can be seen (Fig. 10a) there is only a very small influence of the twist on the ratio between the required torques in and out of the ground effect. On the other hand (Fig. 10b) the increase in the thrust at low heights is greater by more than 30% in the case of the twisted blades.

Conclusions

The results of a new free-wake model of a rotor that hovers in ground effect were presented. The numerical results were compared with experimental data for validation purposes. Very good agreement between thrust coefficients that represent the largest effect was obtained. The ground influence on the required torque was found to be much smaller than on the thrust coefficient, because it is the result of contradicting effects. Also found were relatively large discrepancies between the numerical and experimental torque coefficients. The discrepancies found here, as well as by other researchers, require further investigation.

The numerical model presents good convergence characteristics within the investigated range of all the variables and all the parameters that define the numerical model. Eight cells along the blade and fifteen vortex rings in the far wake give sufficiently accurate results after up to twenty iterations. A more refined model (more cells on the blade, more vortex rings in the far wake etc.) results in a considerable increase in the CPU time and in only negligible changes in the important results. Computer resources can be saved by beginning the computation with a relatively coarse model and by using its converged results to start the calculations with a more refined model. Furthermore, as the ground is approached the number of vortex rings that is needed to represent the far wake can be reduced and thus the required computer resources can be further reduced.

Based on its performance as presented here, the authors feel that this model can be used further to study more aspects of the ground effect on hovering rotors.

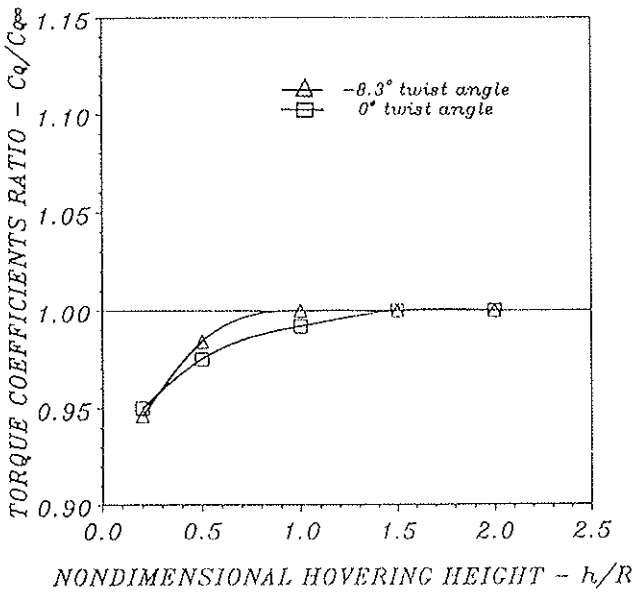

a

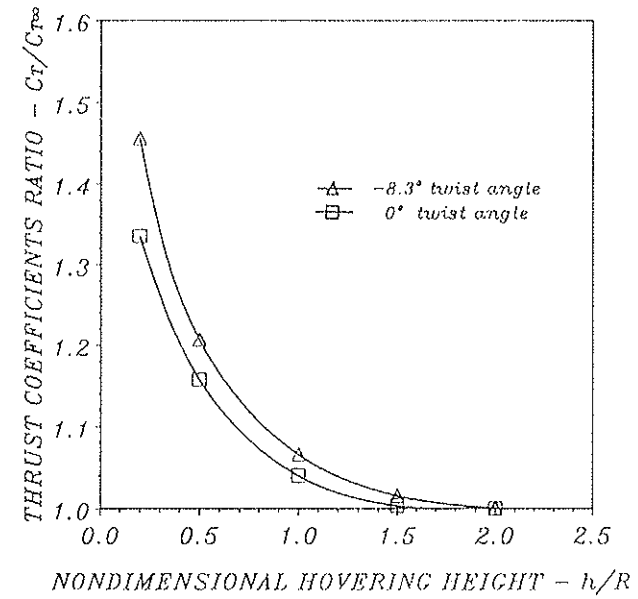

b

Fig. 10. - The influence of the blade twist on the ground effect. (a) Required torque ratio. (b) Thrust ratio.

References

1. Graber, A., Rosen, A. and Seginer, A., "A Free-Wake Model of a Rotor Hovering in Ground Effect", submitted for publication.

2. Rosen, A. and Graber, A., "Free Wake Model of Hovering Rotors Having Straight or Curved Blades", *J. of the American Helicopter Society*, Vol. 33, No. 3, 1988, pp. 11-19.

3. Graber, A. and Rosen, A., "A Parametric Investigation of a Free-Wake Analysis of Hovering Rotors", *Vertica*, Vol. 12, No. 1/2, 1988, pp. 179-196.

4. Saberi, H.A., "Analytical Model of Rotor Wake Aerodynamics in Ground Effect", NASA CR 166533, 1983.

5. DuWaldt, F.A., "Wakes of Lifting Propellers (Rotors) in Ground Effect", Cornell Aeronautical Laboratory, Inc., Buffalo, N.Y. CAL Report No. BB-1655-S-3, 1966.

6. Saberi, H.A., Private Communication, 1985.

7. Graber, A., "A Free-Wake Analysis of Rotor in Ground Effect", D.Sc. Thesis, Faculty of Aerospace Eng., Technion-Israel Institute of Technology, Haifa, Israel, March 1990.

8. Sharpe, D.L., "An Experimental Investigation of the Flap-Lag-Torsion Aeroelastic Stability of a Small-Scale Hingeless Helicopter Rotor in Hover", NASA TP-2546, AVSCOM Tech. Report 85-A-9, 1986.

9. Koo, J. and Oka, T., "Experimental Study on the Ground Effect of a Model Helicopter Rotor in Hovering", NASA TT-F-13938, 1971.

10. Knight, M. and Hefner, R.A., "Analysis of Ground Effect on the Lifting Airscrew", NASA TN-835, 1941.

11. Zbrozek, J., "Ground Effect on Lifting Rotors", A.R.C. Technical Report, R&M No. 2347, 1950.

12. Fradenburgh, E.A., "Aerodynamic Factors Influencing Overall Hover Performance" AGARD-CP-111, "Aerodynamics of Rotory Wings", 1973, pp. 115-125.